

(02)

# In vivo imaging of the mouse retina using high-resolution optical coherence tomography

## *Obrazowanie przyżyciowe siatkówki oka u myszy za pomocą optycznej koherentnej tomografii o wysokiej rozdzielczości*

Anna Machalińska<sup>1,2</sup>, Renata Lejkowska<sup>3</sup>, Michał Duchnik<sup>1</sup>, Dorota Rogińska<sup>3</sup>, Miłosz Kawa<sup>3</sup>, Barbara Wiszniewska<sup>1</sup>

1 Department of Histology and Embryology, Pomeranian Medical University in Szczecin

Head of Department: Professor Barbara Wiszniewska, MD, PhD

2 Department of Ophthalmology, Pomeranian Medical University in Szczecin

Head of Department: Professor Wojciech Lubiński, MD, PhD

3 Department of General Pathology, Pomeranian Medical University in Szczecin

Head of Department: Professor Bogusław Machaliński, MD, PhD

### Abstract:

**Purpose:** In this study, we demonstrate the advantages of high-resolution optical coherence tomography for the non-invasive, *in vivo*, three-dimensional imaging of the mouse retina.

**Methods:** High-resolution optical coherence tomography images of the mouse retina were acquired using the Biotigen Envisu R2200-HR SD-OCT system. We measured the retinal thickness and compared the measurements to those obtained using conventional histology techniques.

**Results:** High-resolution spectral-domain optical coherence tomography enables high-quality *in vivo* visualization of retinal structures in mice, providing an accurate quantitative description of retinal layers. Additionally, the ultra-high-speed system offers many advantages over histology, e.g., it permits the visualization of retinal microvasculature and pulsatile flow dynamics.

**Conclusions:** Spectral domain optical coherence tomography is a new important tool for the *in vivo* analysis of mouse eyes.

### Key words:

spectral-domain optical coherence tomography, retina, blood flow.

### Abstrakt:

**Cel:** w badaniu wykazano zalety optycznej tomografii koherentnej o wysokiej rozdzielczości w przyżyciowym, nieinwazyjnym i trójwymiarowym obrazowaniu siatkówki oka myszy dla celów badawczych.

**Metody:** obrazy o wysokiej rozdzielczości siatkówki oka myszy wykonano metodą spektralnej optycznej tomografii koherentnej, używając systemu Biotigen Envisu R2200-HR. W uzyskanych obrazach przeprowadzono pomiary grubości poszczególnych warstw siatkówki i porównano do tych, które uzyskano z zastosowaniem konwencjonalnych metod histologicznych.

**Wyniki:** spektralna optyczna tomografia koherentna o wysokiej rozdzielczości generuje wysokiej jakości obrazy siatkówki oka myszy. Instrument ten pozwala na dokładną ilościową analizę warstw siatkówki *in vivo*. Ponadto użycie tego systemu przynosi więcej korzyści niż użycie obrazów histologicznych: system umożliwia wizualizację mikrokrążenia siatkówki, ma także funkcję Dopplera, która jest przydatna do ustalenia charakteru przepływu pulsacyjnego.

**Wnioski:** spektralna optyczna tomografia koherentna o wysokiej rozdzielczości jest nowym i innowacyjnym narzędziem do przyżyciowego badania fizjologii i patofizjologii narządu wzroku małych zwierząt laboratoryjnych.

### Słowa kluczowe:

optyczna tomografia koherentna, siatkówka, przepływ krwi.

## Introduction

Optical coherence tomography (OCT) was first reported in 1991 as a non-invasive, cross-sectional ocular imaging technology and today is the most promising noncontact, high-resolution imaging device in ophthalmology (1). OCT uses low-coherence interferometry to detect light echoes, relying on a spectrometer and high-speed camera. Based on the mathematical premise of Fourier transformation it creates the *in vivo* high resolution tomographic images of biological tissues (1, 2). Nowadays, OCT can be regarded as a type of "in-vivo optical biopsy", providing information on retinal pathology *in situ* and in real time, with resolutions close to that of excision biopsy and histopathology. As a result of the enormous progress in this field and develop-

ment of higher-bandwidth illumination which improved the axial resolution to  $\leq 4.0 \mu\text{m}$ , current applications of OCT have been greatly expanded. The launch and subsequent widespread adoption of high-resolution spectral-domain OCT (SD-OCT) created the opportunity for ophthalmology practitioners to attain retinal images of a nearly cellular resolution (3). Moreover, recent advances in three-dimensional image reconstruction have facilitated a better understanding of retinal anatomy. The cellular level *in-vivo* imaging enables clinicians to follow retinal changes over time in patients, which ultimately results in their earlier detection and proper therapeutic intervention.

Similarly, rodent models of retinal diseases provided powerful tools for the analysis and characterization of pathogenesis

in a variety of retinal diseases. Moreover, rat and mouse models have provided the majority of insight into the new therapeutic strategies as well as the retinal response to such novel treatments. Previously, the posterior segment pathology in rodent eye could be examined only by histological preparations of ocular tissue collected *ex vivo*. Accordingly, a large number of animals had to be sacrificed for such type of morphological analysis and particular animal served at only one selected time-point within the experimental study. Therefore, the ability to provide the noninvasive ophthalmic retinal analysis of the living rodent and avoiding the sacrifice of the experimental subject started to be an important aim in longitudinal studies of retinal biology and concurrent pathologic alterations. In contrast, non-invasive imaging techniques make it possible to monitor the retinal tissue over the entire course of disease progression in each individual animal, thus promoting much better understanding of the pathogenesis of a given eye disease in animal model.

The OCT also enables non-invasive visualization of the microscopic anatomy of the rodent retina, however, not without difficulties. The biggest challenge for OCT imaging of the rodent retina is the small size of the eye and its very small pupil. The small pupil size makes the alignment required for light delivery to the eye formidable. It also limits the amount of light reflected from the retina and thus decreases the signal-to-noise ratio (4, 5). Another major obstacle which had to be overcome in mouse OCT imaging was the short focal length of the eye and a very thin retina (6). More recently, high-quality images have been obtained using devices with improved depth resolution that were specifically adapted for particular small animal visual systems. The latest generation of commercially available SD-OCT devices offers scanning speeds and depth resolution sufficient for small animal experimentation. The innovative BiopTigen Envisu R2200-HR SD-OCT system is specifically designed for pre-clinical research and provides high resolution images (1.6  $\mu\text{m}$  axial pixel resolution in tissue). It is equipped with a specialized animal management system, including a stereotactic stage for the rapid alignment of the animal and a real-time exploration, a bite bar for rodent stabilization and an aiming target to ensure the correct working distance.

In this study, we demonstrated the advantages of OCT-based high-resolution imaging of the murine retina. Understanding what is visualized in OCT images requires proper identification of retinal layers and anatomic substructures. Therefore, we measured retinal thickness using the SD-OCT and compared the results to those obtained from conventional histology. We also emphasize the additional benefits of the system, e.g., the ability to visualize the retinal microvasculature and the pulsatile flow dynamics.

### Material and methods

Five pathogen-free 12-month-old male wild-type C57BL6 mice (Polish Academy of Sciences, Wroclaw, Poland), weighing 27–29 g, were used in the experiment. The mice were housed in a standard laboratory environment with a 12-hr/12-hr light-dark cycle at 21°C. For imaging procedures the mice pupils were dilated with 1% atropine. Artificial tears were used throughout the procedure to maintain corneal clarity. Mice were anesthetized with intraperitoneal injection of ketamine (40 mg/kg)

and xylazine (4,0 mg/kg). SD-OCT images were obtained using the Envisu R2200-HR SD-OCT device (BiopTigen, Durham, NC, USA) with the reference arm placed at approximately 1185 mm. Rectangular scans (1.4 mm width, 1000 a-scans/b-scan  $\times$  100 frames/b-scan) were obtained while centered on the optic nerve. SD-OCT scans were imported into InVivoVue Diver (BiopTigen, Durham, NC, USA) to measure the thickness of total retina and retinal layers. For segmentation analysis, we measured manually the total retinal thickness (TR), and the thickness of individual retinal layers: the RPE-photoreceptor complex defined as ranging from Bruch's membrane to the inner limiting membrane (RPE-PR), outer nuclear layer (ONL), outer plexiform layer (OPL), inner nuclear layer (INL) and inner retinal layer (IR) including inner plexiform layer, ganglion cells and nerve fibers. The measurements were taken at 230  $\mu\text{m}$  and 460  $\mu\text{m}$  outward from the center of the optic disk. All retinal measurement procedures in OCT images were performed by one specialized ophthalmologist. Shortly after imaging procedures mice were euthanized by cervical dislocation. For cross-sections, the eyes were paraffin-embedded, cut into 5  $\mu\text{m}$ -thick sections, and stained with hematoxylin and eosin (Sigma-Aldrich, USA). Digital pictures of stained retinal sections were imported into AxioVision digital image processing software (version 4.5.0.0; Carl Zeiss Microimaging, Inc., Thornwood, NY, USA) to manually measure the total retinal thickness and the thickness of the selected retinal layers. All retinal measurement procedures in histological slides were performed by one specialized ophthalmologist. All animal procedures were performed according to the regulations in the ARVO Statement for the Use of Animals in Ophthalmic and Vision Research, and have been approved by the local ethics committee. Student's t-test was used for the statistical analysis of the relationship between the respective retinal thickness measurements.

### Results

Figure 1 shows a single OCT image with all major retinal layers visible. For a comparison, the histological section of the same eye is also shown (Fig. 1a). When analyzing retinal structure *in vivo* using OCT and conventional histology, we observed a significant correspondence between the retinal thickness measurements of specific retinal layers obtained using both imaging techniques (Fig. 1b). However, we also discovered some differences in thickness measurements obtained using SD-OCT and subsequent histological examination of the same retinal layers. The differences were statistically significant in the inner nuclear layer (INL) – (357 vs. 19.4  $\mu\text{m}$ , respectively), outer plexiform layer (OPL) – (12.7 vs. 19.1  $\mu\text{m}$ , respectively) and inner retinal layer (IR) that includes inner plexiform layer, ganglion cells and nerve fibers – (41.7 vs. 71.3  $\mu\text{m}$ , respectively). Thus, we speculate that volume changes resulting from the histological processing of tissue, affected the respective retinal layers to a different extent, thus interfering with our findings. Mismatches encountered when superimposing both histological and OCT images might be due to artifacts arising from tissue handling, such as collapse of blood vessels, or slight deviations of the retinal specimen sectioning plane compared to the plane of the image scan. If the eye cup is not sectioned sagittally along the vertical meridian passing through

the optic nerve, the obtained sections will be slightly oblique and retinal thickness measurements could be inflated. The ability, or inability, to find the exact position at murine eye might determine the accuracy of the lateral registration, and might possibly account for the greatest source of error. We attempted to acquire both SD-OCT images and histological samples through the center of the optic nerve, although the optic nerve was 200 μm wide and it was difficult to identify a section passing through the midline.

An additional benefit of SD-OCT imaging involves the possibility to obtain depth-selective OCT-derived fundus images while retaining ultrahigh resolution. Segmentation algorithms enable precise visualization of retinal layers. By selecting depth and thickness of tissue to be viewed *en face*, it is possible to visualize retinal microvasculature. This allows the detection of small blood vessels and capillaries, e.g. deep vascular bed, just within outer plexiform layer. Figure 2 shows an example

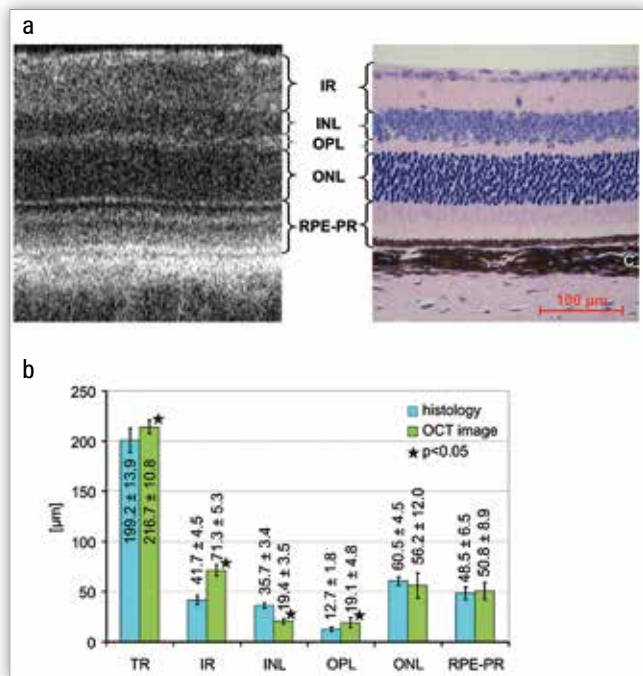


**Fig. 1.** (a) Comparison of the OCT cross-sectional image with a histological section of C57BL6 mouse retina. All intraretinal layers can be identified in the OCT image: RPE-photoreceptor complex (RPE-PR), outer nuclear layer (ONL), outer plexiform layer (OPL), inner nuclear layer (INL), inner retinal layer including inner plexiform layer, ganglion cells, nerve fibres (IR), and choroid (C). (b) SD-OCT measurements performed in murine retinas are compared to histomorphometric data obtained after histological processing of retinas from the same animals.

**Ryc. 1.** (a) Porównanie przekroju siatkówki uzyskanego za pomocą przyżyciowej techniki SD-OCT z przekrojem histologicznym siatkówki u tej samej myszy szczepu C57BL6. Obraz OCT umożliwił identyfikację wszystkich warstw siatkówki: nabłonka barwnikowego siatkówki-fotoreceptorów (RPE-PR), warstwy jądrazstej zewnętrznej (ONL), warstwy spłotowatej zewnętrznej (OPL), warstwy jądrazstej wewnętrznej (INL), warstwy wewnętrznej siatkówki – zawierającej warstwę spłotowatą wewnętrzną, komórki zwojowe, włókna nerwowe (IR), oraz naczyńiówki (C). (b) Porównanie pomiarów grubości poszczególnych warstw siatkówki obrazowanych za pomocą SD-OCT z analizą histomorfometryczną mysich siatkówek pozyskanych od tych samych zwierząt.

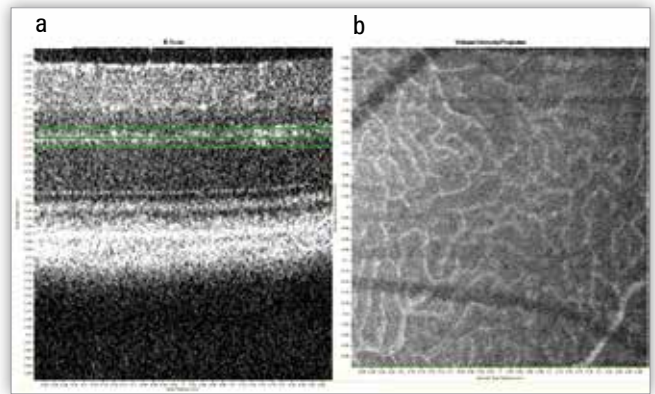


**Fig. 2.** Fundus projection of retinal microvessels. Depth-dependent fundus image visualizes the deep vascular bed just within OPL. Green lines (left) indicate boundaries of tissue depth displayed in *en face* two-dimensional image (right). The right photo shows the vessels above selected layer cast hypodense shadows onto layers beneath. Blood in vessels within a selected layer has a white streaky appearance.

**Ryc. 2.** Zależny od głębokości skanowania obraz dna oka uwidoczniający sieć mikrokrążenia w obrębie warstwy spłotowatej zewnętrznej siatkówki. Zielone linie (zdjęcie po stronie lewej) wytyczają granice tkanki zobrazowanej w projekcji *en face* (zdjęcie po stronie prawej). Na zdjęciu po stronie prawej naczynia znajdujące się powyżej zaznaczonej warstwy rzucają hypodensyjne cienie na warstwy znajdujące się poniżej. Krew znajdująca się w naczyniach w obrębie wybranej warstwy jest hyperdensyjna, widoczna jako białe pasma.

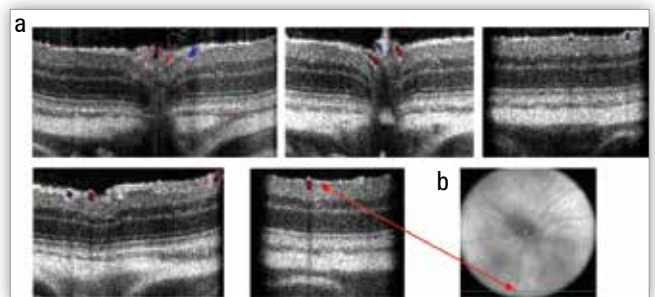


**Fig. 3.** (a) Images showing pulsatile flow in retinal arteries and veins. Differences in the direction of blood flow in exposed blood vessels are marked on the images using color coding – red and blue indicate the reverse direction of blood flow in the adjacent retinal blood vessels. (b) Fundus projection showing the retinal vessel; the same vessel in transverse plane (arrow).

**Ryc. 3.** (a) Obrazowanie przepływu wykazuje obecność pulsacyjnego przepływu w tętnicach siatkówki i powrotu krwi żyłnej w żyłach siatkówki. Odmienny kierunek przepływu krwi w uwidocznionych naczyniach jest zaznaczony na zdjęciach za pomocą kolorowego kodowania kierunku przepływu – kolor czerwony i kolor niebieski wskazują na przeciwstawny kierunek przepływu krwi w sąsiadujących ze sobą naczyniach siatkówki. (b) Naczynie siatkówki uwidocznione na obrazie dna oka oraz to samo naczynie w przekroju osiowym (strzałka).

of the 3D rendering of the volume OCT data. With this method, the retinal microvessels can be visualized with cross-sections at any position and in any direction.

Furthermore, Bioptigen Envisu R2200-HR SD-OCT system also offers the ability to visualize the blood flow in retinal vessels. We were able to detect blood flow within main retinal vessels despite high beam attenuation. The high imaging speed allows detection of pulsatile flow dynamics, distinguishing arteries from veins (Fig. 3).

## Discussion

SD-OCT imaging has several important advantages over the conventional histological studies. The major advantage of OCT is certainly the ability to generate histology-analogue retinal sections *in vivo* as a part of a non-invasive procedure. As we have shown, it may be useful for the assessment of murine retina and enables an accurate quantitative description of the rodent retina layers *in vivo*. It seems that in many cases, the standard histological examination might be replaced or highly reduced by utilizing the SD-OCT technique, thus diminishing the number of experimental animals necessary for the particular research study. Even if histological sections are required, e.g. for immunohistochemical analysis, SD-OCT may help to preselect and to determine the optimal experimental time point for individual animals. It should be mentioned that the same animal retina can be monitored over an extended period of time in order to observe changes in its morphology in the same animal (7).

In contrast, conventional assessment of retinal degeneration relies on histological specimen preparation and light microscopy evaluation, which requires high number of experimental animals, costly embedding materials, days of sample processing, sectioning, and imaging, and many working hours of technicians. Additionally, collecting histologic specimens makes it impossible to perform such studies in the same animal over time. Another problem associated with conventional histology includes visible artifacts, e.g. nonlinear tissue shrinkage and distortions, which may be induced by tissue processing (8, 9). Indeed, the results of our comparative analysis of quantitative measures show that SD-OCT-derived retinal thickness measurements are not exactly identical to those obtained from histology based upon single point measurement performed for each retinal layer. Interestingly, the 4% formaldehyde fixation has been shown to cause volume contraction of whole eyes (10). It should be noted that quantitative measurements using SD-OCT are not completely free of artifacts, either. For example, such optical properties as index of refraction, might vary between retinal layers rich in lipids, thereby altering the scale of thickness measurements. SD-OCT can be used for visualizing changes in optical scattering properties of the tissue or refractive index disruption, but it cannot distinguish between tissues of similar optical properties. By comparison, histology visualizes tissue according to specific staining properties (11). Furthermore, the quality of the OCT image might be severely impaired as a result of even minor corneal opacity, cataracts, and other diseases which may be present in the anterior segment of the eye. Hence, to keep the eye transparent, examination should last as short as possible and artificial tears should be applied to the cornea regularly. Importantly, the propagation of light within tissue is strongly affected by its scattering properties (12).

The additional benefit of SD-OCT imaging is that two-dimensional *en face* projections can be created from the three-dimensional (3D) volume. An *en face* projection of OCT image shows lateral features at each retinal layer. Importantly, in depth-selective OCT-derive fundus images the architecture of retinal microvessels can be clearly seen and situated in true retinal topography.

There is increasing evidence that the pathogenesis of several eye disorders is linked to altered ocular blood flow. The abnormal retinal blood flow occurs in particular in several ocular diseases such as glaucoma, diabetic retinopathy, vascular disorders of the optic

nerve head, and age-related macular degeneration (13). Accurate understanding of ocular perfusion is important not only for disease treatment and management but also for getting insight into the pathophysiology of these diseases. A variety of different techniques have been developed for the retinal blood flow measurement; however, all of them present several important limitations, such as lack of reproducibility in clinical practice or adverse effects (reviewed in detail in: 14). Hence, there is a great demand for the novel methods of ocular vasculature imaging in anatomic detail and for quantitative assessment of blood flow *in vivo*. Likewise, apart from obtaining morphological images, OCT can also detect a Doppler shift of reflected light, which provides information about flow and movement. Doppler OCT (D-OCT) is a functional addition to OCT that facilitates the detection of blood flow in biological tissues, and which provides – in contrast to most other techniques used for blood flow measurement – both structural and functional information (15). Therefore, D-OCT enables evaluation of blood flow and volume in retinal and choroidal vasculature, identification of vessels where the blood flow is present or detecting particular vessel abnormalities (16–18). Currently, D-OCT technique has been used for calculating blood flow in retinal vascular diseases, such as diabetic retinopathy, where the retinal blood flow was shown to be reduced compared to healthy subjects (19). Wang et al. performed the pilot study of D-OCT measurements of retinal blood flow in retinal and optic nerve diseases such as glaucoma, nonarteritic ischemic optic neuropathy, proliferative diabetic retinopathy, and branch retinal vein occlusion. In all investigated disorders, retinal blood flow was significantly decreased compared to healthy eyes (20). Furthermore, in contrast to fluorescein angiography, which is two-dimensional investigation of blood flow, D-OCT may visualize retinal and choroidal vasculature in 3D and calculate the total vessel area (21–23). The Doppler OCT technology, which is currently still in development, may eventually offer significant advantages over the methods used to date for measuring retinal blood flow and help diagnose and monitor progression of different retinal diseases. However, clinical significance of the total retinal blood flow obtained using DOCT has yet to be determined and more extensive studies are needed to validate the clinical application of this new technology.

The system used for studying retinal vasculature BiopTigen Envisu R2200-HR SD-OCT is equipped with Doppler OCT imaging which permits visualization of blood flow and flow dynamics in laboratory animal retinas. Our results show that Doppler OCT detects and visualizes pulsatile flow dynamics of the main retinal arteries and passive venous blood return.

In summary, our results exhibit the SD-OCT device as an important, novel and innovative tool for the *in vivo* analysis of the murine eyes. It emerges as a highly sensitive and totally noninvasive device for monitoring of the morphologic progression of different retinal diseases in rodent models. SD-OCT also appears useful for measuring blood flow and visualizing the main retinal vessels and retinal microvasculature, thus being likely to offer much information for evaluating the nature of retinal structural abnormalities and blood flow abnormalities in different retinal diseases.

Praca finansowana w ramach grantu N N402 665440/  
The research was funded supported by the grant N N402 665440.

**References:**

- Huang D, Swanson EA, Lin CP, Schuman JS, Stinson WG, Chang W, et al.: *Optical coherence tomography*. Science 1991; 254: 1178–1181.
- Drexler W, Sattmann H, Hermann B, Ko TH, Stur M, Unterhuber A, et al.: *Enhanced Visualization of Macular Pathology With the Use of Ultrahigh-Resolution Optical Coherence Tomography*. Arch Ophthalmol. 2003; 121: 695–706.
- Kiernan DF, Mieler WF, Hariprasad S: *Spectral-domain optical coherence tomography: a comparison of modern high-resolution retinal imaging systems*. Am J Ophthalmol. 2010; 149: 18–31.
- Ruggeri M, Wehbe H, Jiao S, Gregori G, Jockovich ME, Hackam A, et al.: *In Vivo Three-Dimensional High-Resolution Imaging of Rodent Retina with Spectral-Domain Optical Coherence Tomography*. Invest Ophthalmol Vis Sci. 2007; 48: 1808–1814.
- Srinivasan VJ, Ko TH, Wojtkowski M, Carvalho M, Clermont A, Bursell SE, et al.: *Noninvasive volumetric imaging and morphology of the rodent retina with high-speed, ultrahigh-resolution optical coherence tomography*. Invest Ophthalmol Vis Sci. 2006; 47: 5522–5528.
- Fischer MD, Huber G, Beck SC, Tanimoto N, Muehlfriedel R, Fahl E, et al.: *Noninvasive, in vivo assessment of mouse retinal structure using optical coherence tomography*. PLoS One. 2009; 4: 7507.
- Ruggeri M, Wehbe H, Jiao S, Gregori G, Jockovich ME, Hackam A, et al.: *In vivo three-dimensional high-resolution imaging of rodent retina with spectral-domain optical coherence tomography*. Invest Ophthalmol Vis Sci. 2007; 48: 1808–1814.
- Knott EJ, Sheets KG, Zhou Y, Gordon WC, Bazan NG: *Spatial correlation of mouse-RPE thickness between SD-OCT and histology*. Exp Eye Res. 2011; 92: 155–160.
- Gloesmann M, Hermann B, Schubert C, Sattmann H, Ahnelt PK, Drexler W: *Histologic correlation of pig retina radial stratification with ultrahigh-resolution optical coherence tomography*. Invest Ophthalmol Vis Sci. 2003; 44: 1696–1703.
- Margo CE, Lee A: *Fixation of whole eyes: the role of fixative osmolarity in the production of tissue artifact*. Graefe's Arch Clin Exp Ophthalmol. 1995; 233: 366–370.
- Muraoka Y, Ikeda HO, Nakano N, Hangai M, Toda Y, Okamoto-Furuta K, et al.: *Real-time imaging of rabbit retina with retinal degeneration by using spectral-domain optical coherence tomography*. PLoS One. 2012; 7: 36135.
- Li Q, Timmers AM, Hunter K, Gonzalez-Pola C, Lewin AS, Reitze DH, et al.: *Noninvasive imaging by optical coherence tomography to monitor retinal degeneration in the mouse*. Invest Ophthalmol Vis Sci. 2001; 42: 2981–2989.
- Flammer J, Orgul S, Costa VP, Orzalesi N, Kriegelstein GK, Serra LM, et al.: *The impact of ocular blood flow in glaucoma*. Prog Retin Eye Res. 2002; 21: 359–393.
- Rechtman E, Harris A, Kumar R, Cantor LB, Ventrapragada S, Desai M, et al.: *An update on retinal circulation assessment technologies*. Curr Eye Res. 2003; 27: 329–343.
- Chen Z, Milner TE, Dave D, Nelson JS: *Optical Doppler tomography imaging of fluid flow velocity in highly scattering media*. Opt Lett. 1997; 22: 64–66.
- Leitgeb RA, Schmetterer L, Hitzenberger CK, Fercher AF, Berisha F, Wojtkowski M, et al.: *Real-time measurement of in vitro flow by Fourier-domain color Doppler optical coherence tomography*. Opt Lett. 2004; 29: 171–173.
- Makita S, Hong Y, Yamanari M, Yatagai T, Yasuna Y: *Optical coherence angiography*. Opt Express. 2006; 14: 7821–7840.
- Miura M, Makita S, Iwasaki T, Yasuno Y: *Three-Dimensional Visualization of Ocular Vascular Pathology by Optical Coherence Angiography In Vivo*. Invest Ophthalmol Vis Sci. 2011; 52: 2689–2695.
- Wang Y, Fawzi A, Tan O, Gil-Flamer J, Huang D: *Retinal blood flow detection in diabetic patients by Doppler Fourier domain optical coherence tomography*. Opt Express. 2009; 17: 4061–4073.
- Wang Y, Fawzi A, Varma R, Sadun AA, Zhang X, Tan O, et al.: *Pilot Study of Optical Coherence Tomography Measurement of Retinal Blood Flow in Retinal and Optic Nerve Diseases*. Invest Ophthalmol Vis Sci. 2011; 52: 840–845.
- Schmoll T, Kolbitsch C, Leitgeb RA: *Ultra-high-speed volumetric tomography of human retinal blood flow*. Opt Express. 2009; 17: 4166–4176.
- Szkułmowska A, Szkułmowski M, Szałg D, Kowalczyk A, Wojtkowski M: *Three-dimensional quantitative imaging of retinal and choroidal blood flow velocity using joint Spectral and Time domain Optical Coherence Tomography*. Opt Express. 2009; 17: 10584–10598.
- Branchini LA, Adhi M, Regatieri CV, Nandakumar N, Liu JJ, Laver N, et al.: *Analysis of Choroidal Morphologic Features and Vasculature in Healthy Eyes Using Spectral-Domain Optical Coherence Tomography*. Ophthalmology 2013 May 9 (Epub ahead of print).

The study was originally received 19.03.2013 (1455)/  
Praca wpłynęła do Redakcji 19.03.2013 r. (1455)  
Accepted for publication 04.02.2014/  
Zakwalifikowano do druku 04.02.2014.

**Reprint requests to (Adres do korespondencji):**

dr hab. n. med. Anna Machalińska  
Klinika Okulistyki SPSK-2  
ul. Powstańców Wlkp. 72  
70-111 Szczecin  
e-mail: annam@pum.edu.pl